Simultaneous Phase, Amplitude, and Polarization Control of Femtosecond Laser Pulses

A. Lindinger, S. M. Weber, M. Plewicki and F. Weise

Institut für Experimentalphysik, Freie Universität Berlin, Arnimallee 14, 14195 Berlin, Germany
E-mail: lindin@physik.fu-berlin.de

Abstract. We present a serial pulse shaper design which allows us to shape the phase, amplitude, and polarization of fs laser pulses independently and simultaneously. The capabilities of this setup are demonstrated by implementing a method for generating parametrically tailored laser pulses. This method is applied on the ionization of NaK molecules by feedback loop optimization, employing a temporal sub pulse encoding. Moreover, we introduce and characterize a further development of this common path pulse shaper scheme for full control of all light field parameters.

INTRODUCTION

The manipulation of the polarization state of femtosecond laser pulses is an emerging topic in the expanding field of coherent control [1]. Such pulses are optimally suited for the interaction with real-world, three-dimensional quantum objects found on the molecular scale [2]. The possibility to control a light field including polarization gives rise to interesting fundamental research applied on different systems [3, 4, 5, 6] The underlying concept of pulse shaping is the manipulation of the frequency components in the Fourier plane of a 4-f line by computer controlled spatial light modulators [7]. The first attempts of shaping the polarization of femtosecond laser pulses were carried out using two liquid crystal modulators without polarizer [8]. This allows for controlling the ellipticity of a polarization ellipse in which the orientation of the principal axis is fixed at 0° or 90°. The unequal reflectivity of the gratings for different polarization components requires compensation which was done with a stack of Brewster plates [9].

Another approach to gain control over the light field is to modulate the horizontal and vertical components separately in phase and amplitude before overlapping them in space and time. This enables unresticted modulation of the light field and was first implemented by incorporating a modulator in a Mach-Zehnder interferometer [10]. This idea was improved by using a Wollaston prism to achieve higher stability in a common optic setup [11]. However, these interferometric designs are still no common path arrangements and hence not entirely stable.

The strategy usually employed to experimentally steer molecular reactions with pulse shapers is to utilize genetic search algorithms [12]. With a parameter-per-pixel encoding, the already vast search space grows even more when appending the polarization. Reducing search space by more general encodings [13, 14], realized for phase and/or amplitude modulation, yields less complex solutions. Moreover, applying parametric shaping of physically relevant pulse features [15] is expected to aid comprehension of the underlying dynamical processes.

In this paper, we first present an analytical approach that produces tailored polarization sub pulse sequences, using a serial setup with a temporal parameter encoding. In the following, we show a polarization enabled coherent control experiment where free and parametric feedback loop optimizations on the ionization of the NaK molecule are compared. Finally, we demonstrate a novel setup in which we use four liquid crystal arrays which allows us to fully control all parameters of the light field, the phase, the amplitude, and the complete polarization state.

PARAMETRIC PULSE FORMING APPROACH

The setup is a serial double-pass arrangement using the commercial CRi SLM-640 Spatial Light Modulator, that the diffracted laser beam passes twice at different locations, effectively employing four arrays at half the resolution (see Fig. 1 (a)). For the first round trip, only the total spectral amplitude is modulated and the possibility to impose phases is disregarded. In the second pass, the spectral phase and polarization are set. The optical axes of the crystals are aligned at 45° and -45° with respect to the incoming, linearly x polarized light (0°). The 4f-setup features cylindrical lenses

International Conference of Computational Methods in Sciences and Engineering 2009
AIP Conf. Proc. 1504, 1275-1278 (2012); doi: 10.1063/1.4772162

with focal lengths of 250 mm and gratings with densities of 600 lines/mm with a reduced polarization dependent reflectivity g, corrected according to Ref. [16]. The laser pulses, produced by an oscillator (Mira, Coherent), have a bandwidth of 22 nm and a central wavelengths of 782 nm. The pulses were detected by sum-frequency-generation cross-correlation (SFG-CC) with a reference pulse in a BBO crystal [10].

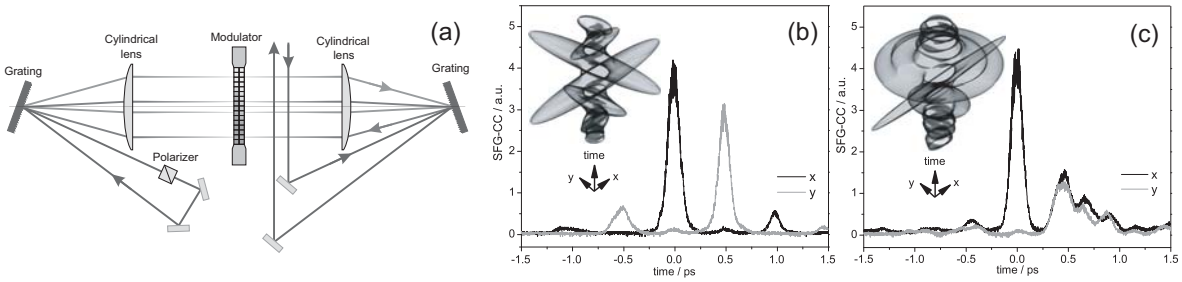

FIGURE 1. (a) Serial shaper configuration. The laser beam enters the first grating, its spectral components are spatially separated, transmitted through the modulator located in the Fourier plane, and hit the second grating. Afterwards the beam is sent through a polarizer and redirected again on the second grating at a different incident angle. The spectral components are sent through a different part of the modulator, reenter the first grating and leave the setup. (b) Double pulse with perpendicular linear polarized sub pulses. (c) Double pulse with a linear and a circular sub pulse with second order chirp. The black (x) and gray (y) lines depict the cross-correlations in horizontal and vertical direction, respectively, and the insets show the 3D representations of the parametric pulse shapes.

An analytic method for producing tailored pulse shapes is presented in the following. The light fields are constructed by assembling several sub pulses having particular parameters including polarization. The sub pulse polarization ellipse parameters intensity I, major axes ratio r, and major axis direction are thereby transformed to the horizontal x and vertical y field amplitudes and their phase shift ε, as shown in Ref. [17], yielding a complex vectorial field after the pulse shaper. The introduced setup (excluding g) is capable of modulating a field described by:

$$\vec{\tilde{E}}_{out}(\omega) = \tilde{E}_{in}(\omega) \cdot R(\omega) e^{\frac{i}{2}(\phi_a(\omega)+\phi_b(\omega))} \begin{bmatrix} \cos\frac{\phi_a(\omega)-\phi_b(\omega)}{2} \\ i\sin\frac{\phi_a(\omega)-\phi_b(\omega)}{2} \end{bmatrix} \tag{1}$$

where $\tilde{E}_{in}$ is the linear input pulse, and ϕ_a and ϕ_b the phase retardances induced by the two second pass shaper arrays. Hence, this setup allows only polarization ellipses with horizontal and vertical principal axes for a given frequency.

The procedure to generate tailored polarization pulse shapes needs solving the system of equations from Eq. 1 for the retardances, which, assuming they are complex, yields $\tilde{\phi}(\omega)_{a,b} = -i\ln[(\tilde{E}_{out,x} \pm \tilde{E}_{out,y})/R(\omega)\tilde{E}_{in}]$ where $+$ and $-$ have to be selected for ϕ_a and ϕ_b, respectively, to obtain the desired $\vec{\tilde{E}}_{out}$. The complex solution for the $\tilde{\phi}(\omega)$ is experimentally not feasible since a single liquid crystal element can not produce an imaginary phase, which would imply amplitude modulation. We instead proceed by using only the experimentally accomplishable real parts of the retardances. In the following we show that this method provides pulses that reasonably represent the desired forms.

Fig. 1(b) shows the x and y component of the SFG-CC traces of two perpendicular linear polarized sub pulses. Their positions were set to 0 and 500 fs and the fluences were chosen to be equal for the sub pulses. The routine yields the intended sub pulse sequence accompanied by perpendicular linear polarized side pulses. Fig. 1 (c) shows the x and y component of the SFG-CC traces of a linear/circular double pulse. Their positions were set to 0 and 400 fs and the fluences were chosen to be equal. The circular pulse, furthermore, has a quadratic chirp of 10^6 fs^3, yielding the characteristic sub pulse train. Simulations of the temporal intensities, calculated by substituting the real parts of the retardances ϕ_a and ϕ_b into Eq. 1, confirms the positions and ellipticities of the main and side pulses in both cases.

OPTIMIZATION OF THE IONIZATION PROCESS IN NAK

The NaK dimers were produced in a molecular beam by adiabatic co-expansion of the metal vapors with argon as a carrier gas (for details see [18]). The conditions were set to produce the molecules mostly in the vibrational ground state. They were detected via a quadrupole mass filter. A Coherent RegA amplifier, seeded by a Coherent Mira, produces pulses with a repetition rate of 100 kHz which is sufficient to ensure that within the interaction region a molecule is not excited more than once. The pulse energies are about 400 nJ per pulse, hence the molecules are

still governed by weak field processes. The evolutionary algorithm employs evolution strategies with 10 parents, 30 offspring, one survivor, and uniform cross-over and self-adapted mutation operators.

We conducted optimizations of the $^{23}Na^{39}K^{+}$ ion yield at a center wavelength of 782 nm with free phase-only modulation, free phase, amplitude, and polarization modulation, and parametric phase, amplitude, and polarization encoding, in order to compare the ionization efficiency and to uncover the effects of polarization modulation. Fig. 2(a) shows the cross-correlation trace of a phase-only optimized pulse with a yield of 1.79 compared to an unshaped pulse. It stands to reason to propose a stepwise excitation scheme for the resulting pulse train as most of the sub pulses can be assigned to multiples of $1/2 \cdot T_{osc}$ = 220 fs of the wave packet in the first excited $^{1}\Sigma^{+}$ state, similar as already reported in Refs. [18, 19]. The result from a free phase, amplitude, and polarization optimization (Fig. 2 (b)) shows a 19% increase to a factor of 2.13 compared to the phase-only case. The cross-correlations in x and y direction can be interpreted as an alternating multi-step excitation, where every linear sub pulse in one direction is followed by another perpendicular one. The sub pulse distances fit well to $1/2 \cdot T_{osc}$ which suggests a repeated stepwise excitation scheme.

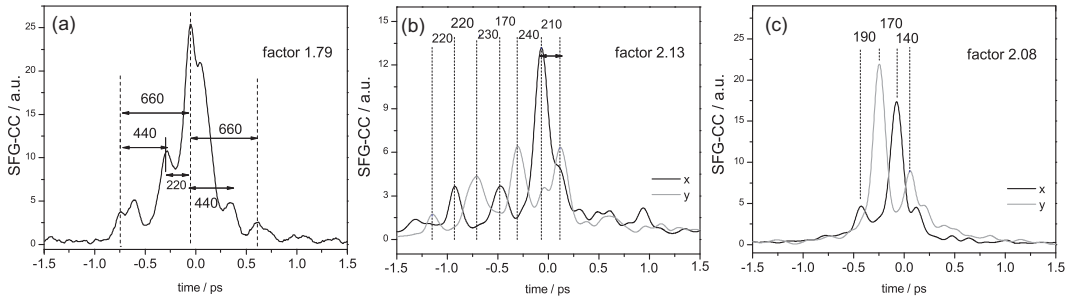

FIGURE 2. Cross-correlation traces of the optimized pulse shapes with free phase-only modulation (a), free phase, amplitude, and polarization modulation (b), and parametric phase, amplitude, and polarization encoding (c). The black (x) and gray (y) lines depict the cross-correlations in horizontal and vertical direction, respectively. The distances are written in fs and the optimization factors are respective to the ion yield of the unshaped pulse.

In an attempt to illustrate the simplification capabilities of parametric shaping we apply the introduced parameterization onto the feedback loop. For the optimizations we again used a double pulse scheme, restricted the major axes angles to 0° and 90°, kept one pulse at time zero and encoded the position of the second major pulse position from -1000 fs to -100 fs. Other parameters were the relative fluences [0.1 to 1], the zero order phases $[-\pi;\pi]$, and the $\Delta\phi$ $[-\pi;\pi]$ of the individual sub pulses. The optimization achieves a total factor of 2.08, see Fig. 2 (c), with a reduced complexity. The pulse shape with alternating perpendicular polarized sub pulses shows similarity with the results from the corresponding free optimization. These results can be understood by the consecutive Σ-Σ to Σ-Π transitions in NaK, having orthogonal transition dipole moments. Hence, the pulse polarization adapts to the transition dipole moments on the optimized path, utilizing the vectorial properties displayed by $\vec{\mu} \cdot \vec{E}$. This demonstrate the perspectives of adding a new dimension by including also the polarization.

FULL CONTROL OF THE LIGHT FIELD

The described pulse shaper is however limited regarding the polarization modulation since the direction of the principle axes of the polarization ellipse cannot be altered. Full control of the polarization can be gained by passing through further liquid crystal arrays, similar to the 8-f setup already reported [20] where yet amplitude modulation is lacking.

Here we demonstrate a novel setup in which we use four liquid crystal arrays in the Fourier plane of a 4-f line which enables us to fully control the four independent degrees of freedom, phase, amplitude, polarization ellipticity, and polarization orientation. This can in principal be done with one modulator consisting of four arrays and one polarizer in between. The first pair of liquid crystal arrays should e. g. be aligned with their optical axis at ±45° to the incoming linearly polarized light followed by a polarizer. This would allow us to modulate the phase and amplitude. The combination of the next array aligned at +45° followed by one at 0° would permit to control the polarization state.

Until now, there are no modulators commercially available with the configuration described above. Therefore, we use three modulators with a double array each (two SLM-640 and one SLM-256, CRi), having their optical axes at ±45°. The first one is used in phase and amplitude configuration with a polarizer behind. The second modulator

provides just one array at -45°, while the second array is set to a constant retardance. In order to obtain an orientation of the optical axis at 0° in the last array, the modulator is placed between two zero order half wave plates at -22.5° each. Again, only one array of this modulator is used. The second wave plate is no constraint but helpful for an intuitive understanding of the formulas and the analytical grating correction.

In order to demonstrate the potential of this setup, we carried out measurements using the Mira oscillator with a spectral width of 28.2 nm at a central wavelength of 781 nm. The whole sequence of the three modulators, the polarizer and the first wave plate is 51 mm thick which, according to test measurements, does not lead to a reduction of the effective shaping resolution.

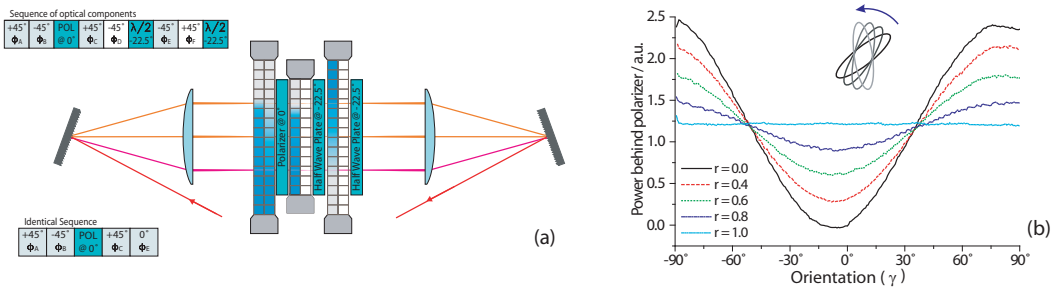

FIGURE 3. (a) Shaper setup consisting of a 4-f line with three double liquid crystal modulators separated by a polarizer and two wave plates at -22.5° in the Fourier plane. (b) Rotation of the ellipse for different r measured behind a vertically aligned polarizer.

To gain intuitive control of the electric field, the parameters $\phi_{a,b,c,e}$ are transformed to the ellipse parameters intensity I, orientation γ, and principal axes ratio r by comparing the equations of the ellipse and the electrical field [10], yielding $\phi_a - \phi_b = 2arccos[\sqrt{I}], \phi_c = 2arctan[g(-1+2(1+r^2)/(1+r^2-(r^2-1)^2cos(2\gamma)))^{1/2}]$, and $\phi_e = -\frac{\pi}{2} + arccos[(2(r^2-1)^2sin(2\gamma)^2)/(1+6r^2+r^4-(r^2-1)^2cos(4\gamma)))^{1/2}]$. In order to analyze the capabilities of the setup, we scanned the polarization ellipse orientation from -90° to +90° at different principal axis ratios while measuring the power transmitted through a polarizer (Fig. 3(b)). These curves exhibit a cosine modulation with decreasing amplitude for increasing r up to circular polarization where a constant signal is observed.

The presented novel pulse shaping setup is the first non-interferometric setup which is capable of modulating the phase, the amplitude, and the full polarization ellipse simultaneously and independently. Accurate control of the ellipse parameters has been demonstrated which will provide the opportunity for unrestricted polarization shaping.

REFERENCES

1. D. Goswami, *Physics Reports* **374**, 385 (2002).
2. Y. Silberberg, *Nature* **430**, 624–625 (2004).
3. T. Brixner, G. Krampert, T. Pfeifer, R. Selle, G. Gerber, M. Wollenhaupt, and *et al.*, *Phys. Rev. Lett.* **92**, 208301 (2004).
4. T. Suzuki, S. Minemoto, T. Kanai, and H. Sakai, *Phys. Rev. Lett.* **92**, 13 (2004).
5. N. Dudovich, D. Oron, and Y. Silberberg, *Phys. Rev. Lett.* **92**, 103003 (2004).
6. M. Aeschlimann, M. Bauer, D. Bayer, T. Brixner, F. de Abajo, W. Pfeiffer, and *et. al.*, *Nature* **446**, 301 (2007).
7. A. M. Weiner, D. E. Leaird, J. S. Patel, and J. R. Wullert, *Opt. Lett.* **15**, 326 (1990).
8. M. M. Wefers, and K. A. Nelson, *Opt. Lett* **20**, 1047 (1995).
9. T. Brixner, and G. Gerber, *Opt. Lett.* **26**, 557 (2001).
10. M. Plewicki, F. Weise, S. M. Weber, and A. Lindinger, *Appl. Opt.* **45**, 8356 (2006).
11. M. Ninck, A. Galler, T. Feurer, and T. Brixner, *Opt. Lett.* **32**, 3379 (2007).
12. R. S. Judson, and H. Rabitz, *Phys. Rev. Lett* **68**, 1500–1503 (1992).
13. T. Hornung, R. Meier, and M. Motzkus, *Chem. Phys. Lett.* **326**, 445–453 (2000).
14. A. Bartelt, C. Lupulescu, Š. Vajda, and L. Wöste, ed. A. Douhal and J. Santamaria, 2002, World Sci. Publishing edn., p. 481.
15. S. M. Weber, A. Lindinger, F. Vetter, M. Plewicki, A. Merli, and L. Wöste, *Eur. Phys. J. D* **33**, 39 (2005).
16. M. Plewicki, S. M. Weber, F. Weise, and A. Lindinger, *Appl. Phys. B* **86**, 259 (2007).
17. S. M. Weber, F. Weise, M. Plewicki, and A. Lindinger, *Appl. Opt.* **46**, 5987 (2007).
18. A. Bartelt, A. Lindinger, S. Vajda, C. Lupulescu, and L. Wöste, *Phys. Chem. Chem. Phys.* **6**, 1679 (2004).
19. B. Schäfer-Bung, R. Mitric, V. Bonacic-Koutecki, A. Bartelt, and *et al.*, *J. Phys. Chem. A* **108**, 4175 (2004).
20. L. Polachek, D. Oron, and Y. Silberberg, *Opt. Lett.* **31**, 631 (2006).